NEW MEASURING METHOD IN ISOTHERMAL TITRATION CALORIMETRY BASED ON A PROPORTIONAL-INTEGRAL CONTROLLED SYSTEM

A. Velázquez-Campoy[1]*, O. López-Mayorga[2] and M. A. Cabrerizo-Vilchez[1]

[1]Departamento de Física Aplicada. Facultad de Ciencias. Universidad de Granada 18071 Granada
[2]Instituto de Biotecnología de la Universidad de Granada, Universidad de Granada 18071 Granada, Spain

Abstract

This paper introduces a new measuring method in Isothermal Titration Calorimetry (ITC). This method, based on a proportional-integral control system, offers many important advantages when compared to the frequently used proportional control: higher signal-to-noise ratio, improved stability of baseline, increased static and dynamic sensitivity, similar or smaller time constants and calibration constant independent of the control parameters.

Here an experimental proof of this method is detailed and full theoretical foundation will be discussed in a next paper.

Keywords: control systems, isothermal titration calorimetry

Introduction

The purpose of this paper is to report on some recent advances in the field of ITC. It deals with a microcalorimeter control system and a new measuring method based on mathematical models of the instrument.

During last decades much attention has been paid to the development of several techniques (harmonic analysis, inverse filtering,...) [1–12] to eliminate or to reduce the distortion (smearing) of the recorded signal produced by the intrinsic thermal inertia of heat flux or conduction calorimeters.

Though it is always possible to accomplish the dynamic correction (deconvolution) of a thermogram, it is far more advantageous to reduce the signal response time, since it is a determining factor for the dynamic sensitivity [13], ex-

---

* Author for correspondence. Fax: +34 58 243214; e-mail: adrianv@goliat.ugr.es

periment duration and time resolution (all of extreme importance when studying complex process, such as e.g. protein adsorption).

It must be pointed out that this signal modification has to be carried out in real time, unlike some deconvolution techniques. It can be done in a fixed configuration scheme by introducing a compensator element that modifies (compensates) the global transfer function and changes the system performance [14–17]. Although it can also be used on line, inverse filtering presents certain intrinsic limitations. Thus, to apply this technique is necessary to know accurately the transfer function of the system; on the other hand, its implementation at analogical level results difficult and rigid, and at digital level, though much more flexible method, it presents the characteristics drawbacks of the digital data processing, specially the introduction of noise associated with derivative operations. The compensation method here proposed, exhibiting the flexibility of the digital filtering, it does not require the knowledge of the system transfer function and it only includes simple digital operations. Therefore, the noise level introduced is smaller.

In order to gain a more insight in the system behaviour using different control methods, mathematical models have been developed which will be fully detailed and discussed in a subsequent paper. The experimental results obtained in the system characterization are in complete agreement with the model predictions. Furthermore, through these models it has been developed a new measuring method based on the proportional integral control (PI). This method offers important advantages when compared to the measuring method based on proportional control (P).

Experimental

At present there are various types of isothermal microcalorimeters available [18–26], but few are those with a high enough sensitivity for protein adsorption studies and they are very expensive. For that reason a differential isothermal titration microcalorimeter with digital control has been designed and constructed in our laboratory, adequate for such research.

Two identical gold cells, sample and reference, are filled with 5 ml of pure water for the calibration operations below described. In each cell, sample and reference, a set of semiconductor thermopiles is used as heat flux sensor (Seebeck effect). They are electrically arranged in series and thermally in parallel, inserted between the outer cell wall and the thermal sink (Fig. 1). The voltage difference between the two flux sensor of the sample and reference cells is amplified (gain ca. 100000, in two stages) (INA103 Burr-Brown) and then digitized by means of a 16-bit A/D converter (DT2805/5716A Data Translation).

In our case compensation is achieved by a digital control system localized in the feedback trajectory consisting of a computer and a 12-bit D/A converter
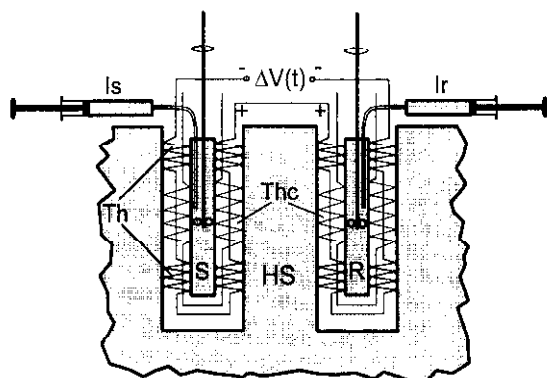
Fig. 1 Schematic diagram of the microcalorimetric unit. S, R – sample and reference cell; Th, Thc – measure and compensation semiconductor thermopiles; Is, Ir – sample and
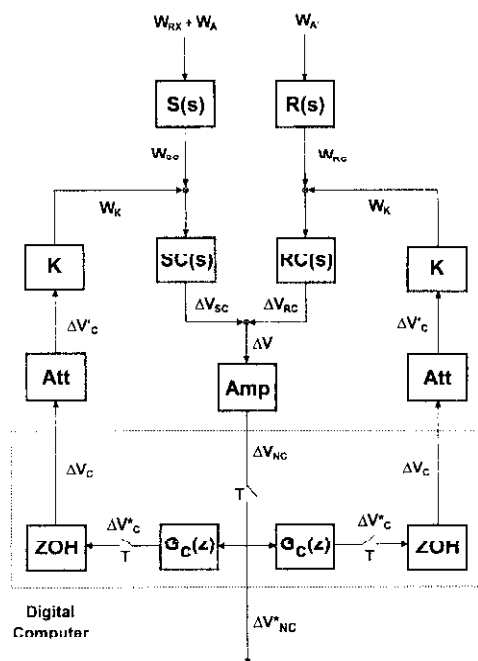

Fig. 2 Block diagram of the microcalorimetric system. S(s), R(s) – transfer function (TF) of sample and reference solution; SC(s), RC(s) – TF of sample and reference cell-sensor ensemble; Amp, Att – TF of amplifier and attenuator; $G_C(z)$ – TF of discrete controller; ZOH, K – TF of zero order holder (DAC) and feedback actuator; W_{RX} – heat power due to chemical reaction or calibration; W_A, $W_{A'}$, – heat power due to thermal artifacts; W_{SC}, W_{RC} – heat power interchanged between solution and cell; W_K heat power generated by feedback actuator; ΔV_{SC}, ΔV_{RC} – voltage generated by heat flux sensor; ΔV – voltage difference between heat flux sensors; ΔV_{NC}, ΔV_{NC}^* – amplified and sampled output signal (non-compensated); ΔV_C, ΔV_C^*, $\Delta V_C'$ – sampled and attenuated feedback signal (compensated)

(DT2805/5176A). The feedback signal is fed into an independent set of thermopiles in each cell. They generate a heat flux (Peltier effect) which attempts to restore thermal equilibrium (baseline). Feedback is produced in a bilateral way. It presents some advantages with regard to the unilateral control, but both are formally identical. So it yields greater symmetry in the system leading to lesser thermal desequilibrium between sample and reference cells; just as minimization of the problem of unilateral Joule heat production by the feedback actuators and equality on the calibration constants for both exothermic and endothermic effects. A block diagram of the calorimeter is shown in Fig. 2. The twin principle is easily identified in the calorimeter design [27].

Control system

The type of control holds the key to the performance of the system. Several controls can be used, but there are some general restrictions on the controls: they must keep the baseline stabilized and the area under the curve followed by the recorded signal must be proportional to the released heat. In other words, the instantaneous signal must be proportional to the heat power which pass through the cell walls. Therefore, there is a non-zero constant response signal for a steady heat effect whose amplitude is proportional to the input heat power. Under this assumptions, the ideal control in this measuring device is the one that permits big baseline deflections when heat is being evolved (good signal-to-noise ratio) and secures a fast return to equilibrium (baseline), i.e. the system has high steady-state gain and small time constants. As will be seen later, these two conditions are in conflict when a P control is used. but the PI control allows a better approaching to the ideal control.

The control element is represented by its transfer function, $G_C(z)$, where $z = \exp(Ts)$ and s is the Laplace Transform parameter. A discrete or pulsed transfer function is used because the controller is a digital computer sampling the signal with a period T. Flexibility and easiness of implementation of digital controls when compared to analogical ones have been taken into account.

Three possible cases can be considered:

a) In the non controlled system there is no feedback loop and, consequently, the feedback signal ΔV_C and transfer function $G_C(z)$ are null:

$$\Delta V_C(kT) = 0 \qquad \text{(time domain)}$$

$$\Delta V_C(z) = 0 \qquad \text{(frequency domain)} \qquad (1)$$

$$G_C(z) = 0 \qquad \text{(frequency domain)}$$

where k is a time counter.

b) In the P-controlled system:

$$\Delta V_C(kT) = K_P \Delta V_{NC}(kT) \quad \text{(time domain)}$$

$$\Delta V_C(z) = K_P \Delta V_{NC}(z) \quad \text{(frequency domain)} \tag{2}$$

$$G_C(z) = K_P \quad \text{(frequency domain)}$$

where ΔV_{NC} is the output signal and K_P is the proportionality constant.

c) And in the PI-controlled:

$$\Delta V_C(kT) = K_P \Delta V_{NC}(kT) + K_1 \sum_{k'=1}^{k'=k} T \frac{\Delta V_{NC}(k'T) + \Delta V_{NC}((k'-1)T)}{2} \quad \text{(time domain)}$$

$$\Delta V_C(z) = \left(K_P + K_1 \frac{Tz+1}{2z-1} \right) \Delta V_{NC}(z) \quad \text{(frequency domain)} \tag{3}$$

$$G_C(z) = K_P + K_1 \frac{Tz+1}{2z-1} \quad \text{(frequency domain)}$$

where K_1 is the integration constant.

The control algorithms implemented are followed from the last expressions:

$$\Delta V_C(kT) = 0$$

$$\Delta V_C(kT) = K_P \Delta V_{NC}(kT) \tag{4}$$

$$\Delta V_C(kT) = \Delta V_C((k-1)T) + \left(\frac{K_1 T}{2} + K_P \right) \Delta V_{NC}(kT) + \left(\frac{K_1 T}{2} - K_P \right) \Delta V_{NC}((k-1)T)$$

respectively, for the non controlled, P-controlled and PI-controlled system. In the last case, instead of forward or backward approximation, the trapezoidal one is used, since it yields better results [28]. In these equations, K_P and K_1 are the control parameters.

In the non controlled system the non compensated signal is proportional to the heat flux passing through the cell when a thermal effect takes place. Likewise, as it will be shown [29], in the P-controlled system both non compensated and compensated (feedback) signals are proportional to the heat flux. However, in the PI-controlled system only the feedback signal shows this proportionality. This stems from the following fact: in the two first systems the open loop transfer function is of type 0 (it has no poles at $z=1$) and in the third one of type 1 (it has a pole at $z=1$). So, the steady-state value of the non compensated signal for the response to a power step becomes different to zero in the first case and zero in the second case. However, the feedback signal behaves in similar way for P and PI control, showing a non zero steady state value. This is illustrated by Fig. 3.
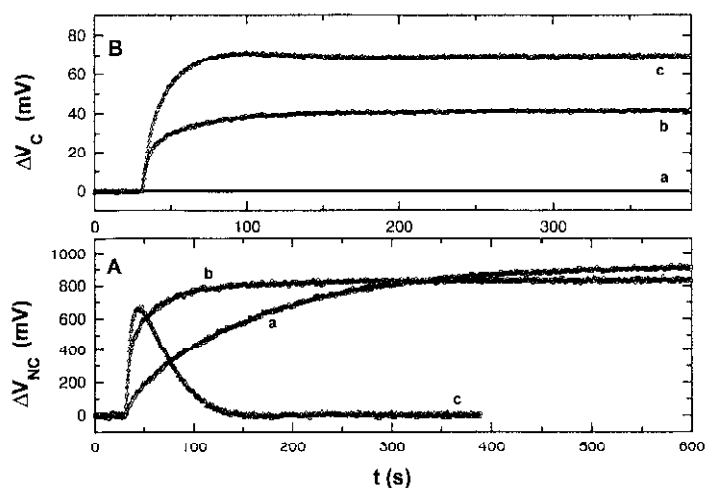
Fig. 3 Calorimetric response to a power step: a) without control; b) P control, c) PI control. Panel A: non-compensated (output) signal, Panel B: compensated (feedback) signal

Results and discussion

Firstly, we will analyze individually the behaviour of each system. Then, a comparison will be made between the two control systems. It is obvious that the non controlled system is a particular case of the other ones (K_P=0 and K_I=0).

The experiments consist of electrical calibrations carried out by passing a definite electrical current through a resistor (161.94 Ω) made of 'molecular wire'
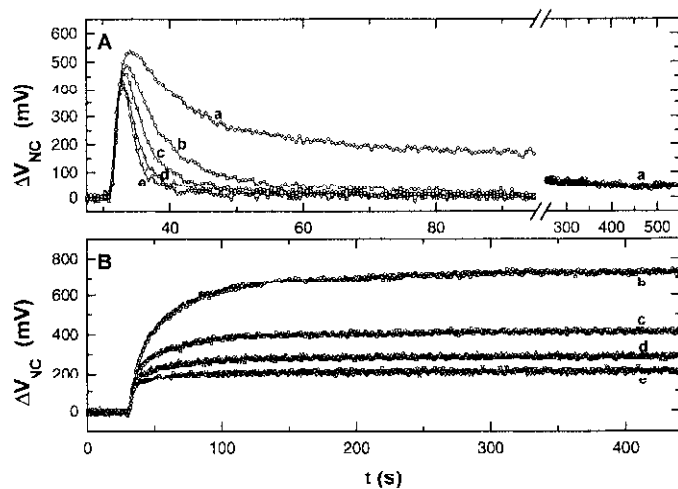

Fig. 4 Influence of K_p on the calorimetric response. a) K_p=0; b) K_p=0.025; c) K_p=0.05, d) K_p=0.075; e) K_p=0.1. Panel A: response to pulse input (717 μW during 1 s), Panel B: response to step input (84 μW)

wound around the sample cell wall. A programmable power supply (Keithley 220 Programmable Current Source) was used for this purpose.

a) P Control

The two standard input signals to analyze the behaviour of a calorimeter are a heat pulse (of finite width) and a power step [30–31]. The non compensated signal corresponding to such inputs are illustrated in Fig. 4, showing as well the influence of the K_P parameter on the performance of the calorimeter. Clearly it is observed that the response becomes faster for increasing K_P values, however the area under the curve for pulse response and the steady-state limit for the step response decrease strongly. Moreover there is a reduction in signal-to-noise ratio because the noise level does not change appreciably. For greater values of K_P the peaks are better defined and the errors due to drift of the baseline are minimized.
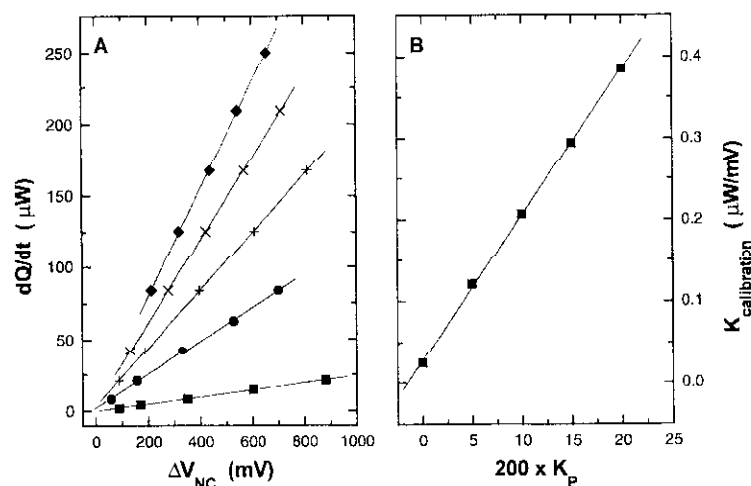

Fig. 5 Influence of K_p on the calibration constant. Panel A: heat power vs. non-compensated signal for different K_p values. The calibration constants are obtained from the slope of the linear regressions, ■ – K_p=0, ● – K_p=0.025, + – K_p=0.05, x – K_p=0.075, ♦ – K_p=0.1. Panel B: Dependence of calibration constant on K_p

According to the reduction in area and steady-state limit, a variation of the calibration constant, $K_{calibration}$ with increasing K_P parameter is observed. This dependence is illustrated in Fig. 5. In Panel A five sets of different heat powers for different values of K_P are shown. The calibration constant can be calculated with linear regression of these data. The resulting values and their corresponding standard error, $\delta K_{calibration}$, are summarized in Table 1. Panel B of Fig. 5 displays the dependence of calibration constant on K_P. It must be emphasized that the linearity of the calibration constant is in complete agreement with the theoretical prediction [29].
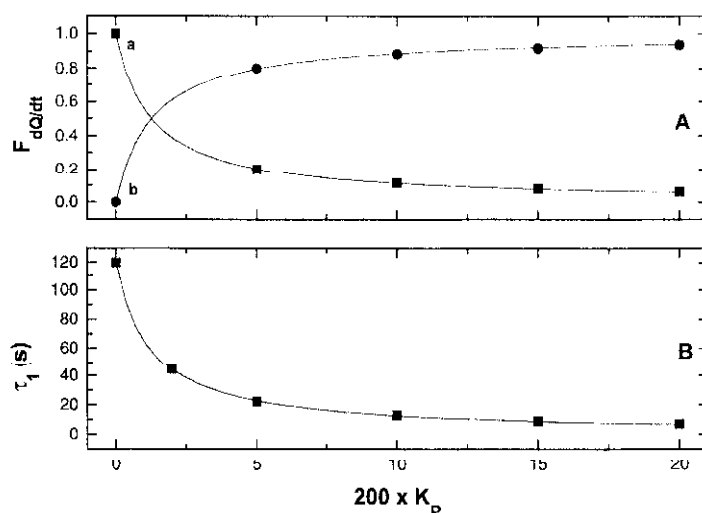
Fig. 6 Panel A: influence of K_p on the compensated and non-compensated heat fraction.
Panel B: influence of K_p on the time constant of the calorimeter

Assuming that the calorimeter can be approximated by a first-order system (this is true when an electrical calibration on the cell wall is done), the time constant, τ_1, and its estimated error, $\delta\tau_1$, can be obtained. A trend completely consistent with the model derivations appears (Fig. 6, Panel A). Moreover, the product of the calibration constant by the time constant remains nearly constant, as predicted by the model [29] [32] (Table 1).

Table 1 Calibration contants and time constants

K_p	$K_{calibration}/$ $\mu W\ mV^{-1}$	$\delta K_{calibration}$	$\tau_1/$ s	$\delta\tau_1$	$K_{calibration}\ \tau_1/$ $\mu W\ s\ mV^{-1}$	$\delta(K_{calibration}\ \tau_1)$
0.000	0.024	0.0003	120	1	2.9	0.3
0.025	0.121	0.002	22	1	2.7	0.1
0.050	0.207	0.002	13	1	2.7	0.2
0.075	0.295	0.002	9	1	2.7	0.2
0.100	0.384	0.002	7	1	2.7	0.2

In the P-controlled system there are two signals carrying information, ΔV_{NC} and ΔV_C. They are associated with heat powers W_{NC} and W_C. It must be obeyed that:

$$W_T = W_{NC} + W_C \tag{5}$$

$$Q_T = Q_{NC} + Q_C$$

where W_T is the global heat power released in the cell and Q_{NC}, Q_C and Q_T are the corresponding heats which they can be calculated by means of the next relationship:

$$Q_T = K_{calibration} \int_{t_0}^{t_f} \Delta V_{NC}(t)dt \equiv K_{calibration} T \sum_{k=k_0}^{k=k_f} \Delta V_{NC}(kT) = K_{calibration} Area_{NC} \qquad (6)$$

$$Q_{NC} = K_{calibration}|_{K_P=0} Area_{NC} \qquad (7)$$

where $Area_{NC}$ is the area under de recorded curve $\Delta V_{NC}(t)$.

At this point, the compensated and non-compensated heat fraction can be defined as follows:

$$F_{NC} = \frac{Q_{NC}}{Q_T} \qquad F_C = \frac{Q_C}{Q_T} = 1 - F_{NC} \qquad (8)$$

These fractions are represented graphically in Fig. 6 (Panel B) and we can observe that for low K_P values these fractions show strong change and for high K_P values they hardly change at all. With increasing K_P it becomes more difficult to increase the compensation fraction and, in fact, is impossible to obtain a compensation fraction of 1.0 as this would make the system oscillatory and unstable.

b) Control PI

Similarly, in Figs 7 and 8 the responses under PI control to a heat pulse and a power step are depicted. It can be easily recognized how K_P and K_I influence on the response features. Here follows a summation.

• The noise level is determined by K_P.
• As K_I increases, the damping coefficient decreases.
• For fixed K_P, the time constant decreases slightly with increasing K_I.
• For increasing K_P and K_I there is no reduction in the area for heat pulses nor in the steady-state limit value for power steps. This suggests that the calibration constant does not depend on the control parameters K_P and K_I, leading to a signal-to-noise ratio decreasing only due to the increasing noise level.
• For higher values of K_P the peaks are sharper (identical area but narrower).
• For fixed K_P, there is a critical $K_{I,crit}$ value for which: if $K_I > K_{I,crit}$ the system is oscillatory and if $K_I < K_{I,crit}$ the behaviour is not so. Furthermore, this critical value increases with increasing K_P.
• Since the area under the curve for a heat pulse input and the steady-state value for a power step input are zero for the non-compensated signal, the compensated fraction is 1.0 and the non-compensated fraction is zero. In practice $Area_{NC}$ has values close within its error.

It is very important to emphasize that all of these observations are in complete agreement with the theoretical model [29].
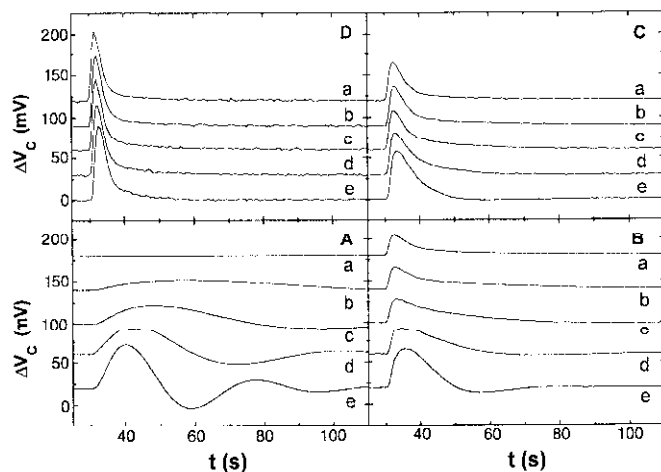
Fig. 7 Influence of K_p and K_i on the response to a heat pulse input (1438 µW during 1 s).
A) K_p=0; B) K_p=0.025; C) K_p=0.05; D) K_p=0.1, a) K_iT=0; b) K_iT=0.0005;
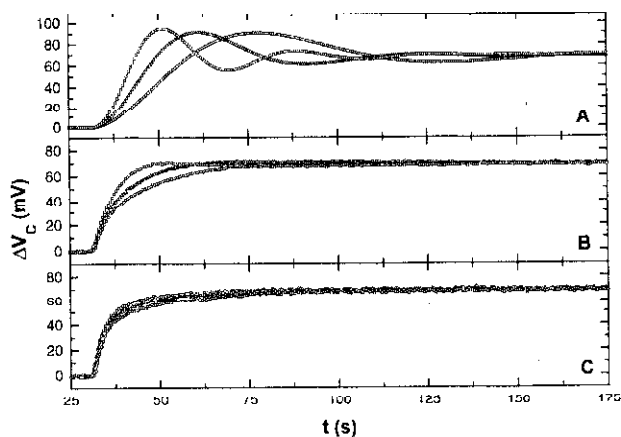c) K_iT=0.00125; d) K_iT=0.0025; e) K_iT=0.005

Fig. 8 Influence of K_p and K_i on the response to a power step input (247 µW).
A) K_p=0; B) K_p=0.05, C) K_p=0.1. o − K_iT–0.00125; Δ − K_iT–0.0025, □− K_iT=0.005

c) Comparative study

The previous analysis was aimed at finding the characteristics of each control system. So, a comparison can be made.

It must be pointed out that under PI control the compensated heat fraction, unlike the P control, reaches the limit value of 1.0. If it is tried out with the P control the calorimeter becomes oscillatory and unstable.

From Eqs (2) and (6) one can obtain a simple relationship between the calibration constants for both non compensated and feedback signals for the P control system:

$$K^{\text{C}}_{\text{calibration}} = \frac{K_{\text{calibration}}}{K_{\text{P}}} \tag{9}$$

where $K_{\text{calibration}}$ and $K^{\text{C}}_{\text{calibration}}$ are the calibration constants when ΔV_{NC} and ΔV_{C} are the measured signals considered, respectively.

Table 2 Calibration constant for compensated signal

K_{P}	$K^{\text{C}}_{\text{calibration}}/$ $\mu W\ mV^{-1}$ *	$\delta K^{\text{C}}_{\text{calibration}}$ *	$K^{\text{C}}_{\text{calibration}}/$ $\mu W\ mV^{-1}$ **	$\delta K^{\text{C}}_{\text{calibration}}$ **
0.000	–	–	3.45	0.01
0.025	4.84	0.08	3.45	0.01
0.050	4.14	0.04	3.44	0.01
0.075	3.93	0.03	3.44	0.01
0.100	3.84	0.02	3.44	0.01

*P control; ** PI control

Table 3 Noise level

K_{P}	$\text{noise}_{\text{NC}}/mV$ *	$\text{noise}_{\text{C}}/mV$ *	$\text{noise}_{\text{C}}/mV$ **
0.000	6.1	–	0.06
0.025	6.3	0.16	0.14
0.050	7.0	0.35	0.30
0.075	7.1	0.54	0.49
0.100	7.3	0.74	0.68

*P control; ** PI control

Table 4 Signal-to-noise ratio

K_{P}	$\text{SNR}_{50\mu W}$ *	$\text{SNR}_{50\mu W}$ **
0.000	341.6	230.1
0.025	65.6	103.5
0.050	34.5	48.5
0.075	23.8	29.7
0.100	17.8	21.5

*P control; ** PI control

Carrying out a non linear fit of the $K_{calibration}^C$ values as function of K_P (Table 2), a limit $K_{calibration}^C$ value of 3.49±0.02 is obtained for K_P tending towards infinity, which is very close to the calibration constant in the PI-controlled system.

It can be clearly seen in Table 3 that the proportional-integral algorithm has a notable effect smoother, since the noise level (standard deviation of the signal) is appreciably reduced.

In Table 4 values of signal-to-noise ratio, SNR, for response to a 50 µW power step input are indicated. The improvement due to the PI control can be observed: for the two controls SNR decreases with decreasing K_P, but faster for the P control. Here this ratio is defined as follow:

$$SNR = \frac{(\Delta V_C)}{\sigma_{\Delta V_C}} \qquad (10)$$

where (ΔV_C) and $\sigma_{\Delta V_C}$ are the averaged value and the standard deviation of the compensated signal calculated for an interval of 60 s.
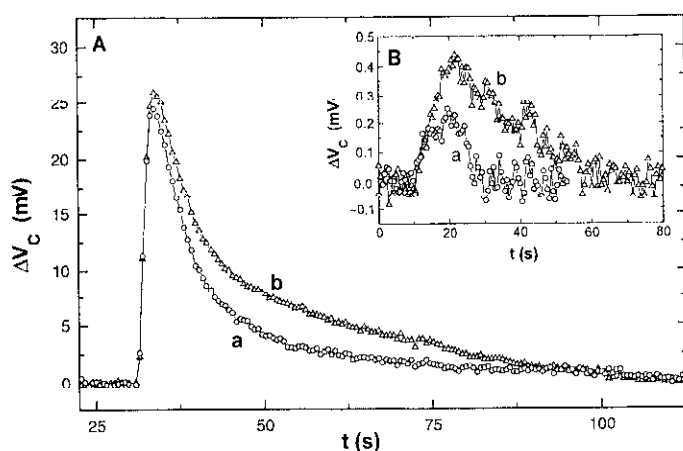

Fig. 9 Comparative plots of a heat pulse response under P and PI control. a) K_p=0.025; K_iT=0; b) K_p=0.025; K_iT=0.0005. Panel A: 1438 µW during 1 s, Panel B (inset): 8.4 µW during 10 s

Finally, in Fig. 9 the improved sensitivity of the PI control is illustrated. For a given heat pulse, there is a larger area under the curve with no change in time lag to reestablish baseline. This fact stems from its higher signal-to-noise ratio with regard to the P control.

Conclusions

The PI control can be considered as the limit case for K_P tending towards infinity of the P control (situation physically impossible to reach in the P control).

This may be inferred from both the experimental evidence and the mathematical treatment [29].

The most important conclusion is that a PI control improves the performance of the calorimeter. The main improved features are:

i) larger signal-to-noise ratio,

ii) compensation fraction equals unity,

iii) higher static and dynamic sensitivity,

iv) similar or smaller time constants,

v) calibration constant insensitive to control parameters.

*   *   *

References

1 J. L. Macqueron, J. Ortín, G. Thomas and V. Torra, Thermochim. Acta, 67 (1983) 213.

2 J. Ortín, A. Ramos, V. Torra, J. Viñals, E. Margas and W. Zielenkiewicz, Thermochim. Acta, 76 (1984) 325.

3 J. Hatt, E. Margas and W. Zielenkiewicz, Thermochim. Acta, 64 (1983) 305.

4 S. Tanaka, Thermochim. Acta, 25 (1978) 269.

5 S. Tanaka, Thermochim. Acta, 156 (1989) 117.

6 C. Rey, J.R. Rodríguez and V. Pérez-Villar, Thermochim. Acta, 61 (1983) 1.

7 E. Cesari, V. Torra, J. L. Macqueron, R. Prost, J. P. Dubes and H. Tachoire, Thermochim. Acta, 53 (1982) 1.

8 E. Cesari, V. Torra, J. L. Macqueron, R. Prost, J. P. Dubes and H. Tachoire, Thermochim. Acta, 53 (1982) 17.

9 J. Ortín, V. Torra, J. Viñals and E. Cesari, Thermochim. Acta, 70 (1983) 113.

10 E. Cesari, J. Ortín, P. Pascual, V. Torra, J. Viñals, J. L. Macqueron, J. P. Dubes and H. Tachoire, Thermochim. Acta, 48 (1981) 367.

11 G. W. H. Höhne, Thermochim. Acta, 22 (1978) 347.

12 J. R. Rodríguez, C. Rey, V. Pérez-Villar, V. Torra, J. Ortin and J. Viñals, Thermochim. Acta, 63 (1986) 331.

13 E. Margas and W. Zielenkiewicz, Thermochim. Acta, 215 (1993) 9.

14 B.C. Kuo, Digital Control Systems, 2nd De., Saunders College Publishing, U.S.A. (1992).

15 S. L. Randzio, Thermochim. Acta, 44 (1981) 1.

16 R. Ambrosetti, N. Ceccanti and C. Festa, J. Phys. E: Sci. Instrum. , 16 (1983) 265.

17 O. López-Mayorga, P. L. Mateo, J. Mira and M. Cortijo, J. Phys. E. Sci. Instrum., 17 (1984) 1231.

18 E. Freire, O. López-Mayorga and M. Straume, Anal. Chem., 62 (1990) 950A.

19 M. El-Harrous, S. J. Gill and A. Parody-Morreale, Meas. Sci. Technol., 5 (1994) 1065.

20 M. L. McGlashan, Thermochim. Acta, 72 (1984) 55.

21 I. Wadsö, Thermochim. Acta, 169 (1990) 151.

22 L. D. Hansen and D. J. Eatough, Thermochim. Acta, 70 (1983) 257.

23 H. Huemer, E. Platzer and K. Rehak, Thermochim. Acta, 231 (1994) 21.

24 I. Wadsö, Thermochim. Acta, 96 (1985) 313.
25 T. Wiseman, S. Williston, J. F. Brandts and L. Lin, Anal. Biochem., 179 (1989) 131.
26 J. Rouquerol, Thermochim. Acta, 96 (1985) 377.
27 J. Barthel, Thermometric Titrations, Ed. John Wiley & Sons, USA (1975).
28 J. R. Leigh, Applied Digital Control: Theory, Design and Implementation, 2nd Ed., Prentice Hall International, UK (1992).
29 A. Velázquez-Campoy, O. López-Mayorga and M. A. Cabrerizo-Vílchez, to be published.
30 K. R. Löblich, Thermochim. Acta, 231 (1994) 7.
31 J. P. Dubes, R. Kechavarz and H. Tachoire, Termochim. Acta, 79 (1984) 15.
32 O. López-Mayorga, P. L. Mateo and M. Cortijo, J. Phys. E: Sci. Instrum., 20 (1987) 265.